Advances in Military Technology
Vol. 21, No. 1, 2026, pp. 129-139
ISSN 1802-2308, eISSN 2533-4123
DOI 10.3849/aimt.01903

Calculation of Recoilless Weapons with a High-Pressure Chamber

D. Quoc Vi[1], N. Trang Minh[1], V. Minh Do[2], D. Dung Tran[3*], M. Macko[3], V. Dung Bui[3], L. Minh Duc[4], and N. Sy Tien[4]

[1] *Academy of Military Science and Technology, Hanoi, Vietnam*
[2] *Department of Weapons, Le Quy Don Technical University Technology, Hanoi, Vietnam*
[3] *University of Defence, Brno, Czech Republic*
[4] *Weapon Institute, Vietnam Defence Industry, Hanoi, Vietnam*

The manuscript was received on 22 May 2024 and was accepted after revision for publication as an original research paper on 23 March 2026.

Abstract:

This paper presents an internal ballistics model for recoilless weapons in which the propellant gas flows out from the high-pressure chamber (HPC). The problem is solved using the numerical integration method in MATLAB software. The mathematical model and experiment were used to determine the gas pressure in the HPC, low-pressure chamber (LPC), time and velocity of the grenade at the muzzle. The maximum difference between the results of the mathematical model and experimental data was found to be 7.92 % for both cases, where the initial temperatures of the propellant charge were set at 5 °C and 50 °C.

Keywords:

recoilless weapons, internal ballistics, high-pressure chamber

1 Introduction

High-pressure chambered recoilless weapons are commonly used in anti-tank and grenade launcher weapons (Fig. 1). The advantage of this weapon is that the propellant charge burning in HPC is more stable. On the contrary, the gas pressure in LPC, which forces the grenade to move, is not high, resulting in unstable burning of the propellant charge. The propellant gas flowing to the rear creates an impulse that is in the opposite direction to the recoil of the weapon. This propellant gas may flow from HPC, LPC or both. As a result, the force acting on both the grenade and the barrel is low, the weapon is highly mobile, compact in design, easy to use and suitable for personal use [1-5].

* *Corresponding author: Department of Weapons and Ammunition, University of Defence, Kounicova 156/65, CZ-662 10 Brno, Czech Republic. E-mail: dinhdung.tran@unob.cz. ORCID 0009-0000-1207-8460.*

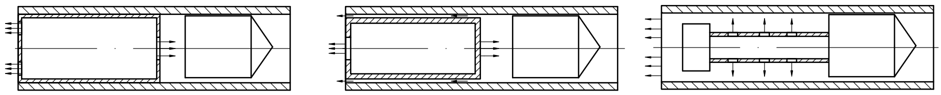

Fig. 1 The schematic diagram of a recoilless weapon with a HPC
a) flowed out from HPC; b) flowed out from HPC and LPC; c) flowed out from LPC

These types of weapons combine conventional weapons with rocket engines. Several studies have been conducted on HPC weapons, including studies [6-9] that have successfully addressed the issue of the internal ballistics of these weapons. However, the models of these studies do not simultaneously consider factors such as:

- initial temperature of propellant charge and igniter charge,
- the combustion of igniter charge in the igniter tube,
- the gas exchange between the igniter tube and HPC,
- gas leakage through the gap between the grenade and the firing tube.

The combustion process of igniter charge and the gas exchange between the igniter tube and HPC play a crucial role in ensuring the reliable ignition of the propellant charge. Additionally, the influence of the initial propellant charge temperature on muzzle velocity and gas pressure should be carefully considered. By developing an internal ballistic model that accounts for these factors, designers can investigate and select optimal parameters such as igniter charge mass, igniter tube size, vent hole area, igniter tube material, and evaluate weapon performance under various environmental temperatures.

The work [9] by the authors has developed a system of equations for recoilless weapons in which the propellant gas flows out from HPC, using calculation data for a 93mm recoilless weapon with initial propellant temperature of 50 °C. The results for muzzle velocity, maximum pressure in HPC, and LPC are consistent. However, the model does not account for factors such as: the initial temperature of the propellant and igniter charge, the combustion of the igniter charge in the igniter tube, the gas exchange between the igniter tube and HPC, and gas leakage through the gap between the grenade and the barrel.

Extending the earlier work in [9], this study introduces additional mathematical equations to consider the influence of the aforementioned factors. Experiments were conducted to validate the developed mathematical model of internal ballistics for both cases, where the initial temperatures of the propellant charge were set at 5 °C and 50 °C.

2 Theoretical Model

2.1 Principle of Operation of Recoilless Weapons with HPC

A schematic illustration of the internal ballistic cycle of a HPC recoilless weapon is shown in Fig. 2.

The firing process begins when the igniter charge in the igniter tube is ignited. The fuse burns at a constant volume until the gas pressure reaches a value at which the seal is broken. As the vents open, propellant gas flows into HPC, igniting the propellant charge. Combustion then proceeds at a constant volume within HPC until the gas pressure reaches the required levels for nozzles 1, 2, and 3, respectively. In this sequence, nozzles 1, 2, and 3 are opened. Propellant gas flows through nozzle 1 into LPC and exits into the atmosphere via nozzles 2 and 3. The grenade begins to move once the gas pressure in LPC reaches the "starting pressure".

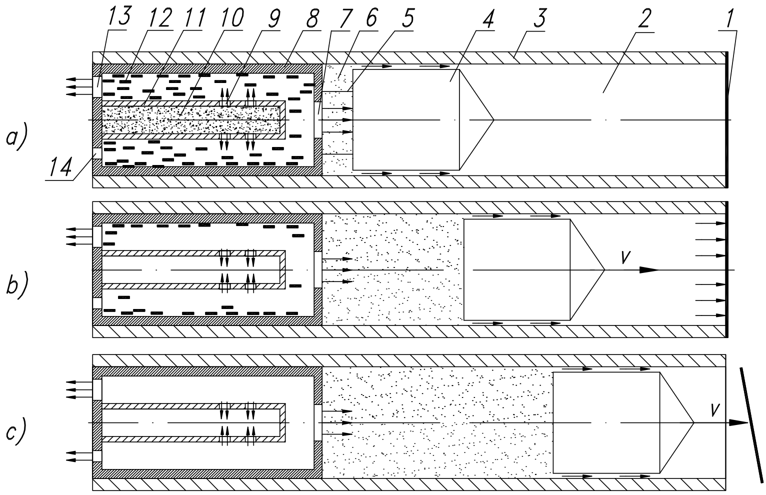

Fig. 2 The scheme of a recoilless weapon with a HPC in the case of propellant gas flowing out from HPC: 1. Cap; 2. Chamber N. 4; 3. Launcher tube; 4. Grenade; 5. Joint; 6. Low-pressure chamber; 7. Nozzle 1; 8. HPC; 9. Vents; 10. Igniter charge; 11. Igniter tube; 12. Propellant charge; 13. Nozzle 2; 14. Nozzle 3

2.2 Mathematical Model

The internal ballistic mathematical model is developed based on the following important assumptions [1-6, 8-9] (see in [9]). In the mathematical model for this study, two important assumptions are omitted: "the igniter charge burns instantaneously" and "ignoring the gap between the grenade and the barrel". At time $t = 0$, the pressure in both HPC and LPC is equal to the ambient pressure.

The new system of equations includes propellant charge burning, equation of gas flowing out, equation of mass, equation of energy, equation of state, equation of grenade moving in HPC and LPC that have been developed [9], along with newly constructed equations (the equations in the igniter tube and equations for gas flow through leakage between grenade and barrel).

Due to the addition of new equations to the original system, some equations will be modified, such as the energy, mass, and state equations of HPC and LPC. The equations of the new mathematical model are as follows:

The equations in igniter tube:

- propellant charge burning

$$\frac{\mathrm{d}z_1}{\mathrm{d}t} = \frac{\left[1 - k_{\mathrm{t1}}\left(T_{\mathrm{bd}} - T_{\mathrm{tc1}}\right)\right]^{-1}}{I_{\mathrm{k1}}} p_1 \tag{1}$$

$$\frac{\mathrm{d}\psi_1}{\mathrm{d}t} = \chi_1\left(1 + 2\lambda_1 z_1 + 3\mu_1 z_1^{\,2}\right)\frac{\mathrm{d}z_1}{\mathrm{d}t} \tag{2}$$

- equation of gas flowing out between igniter tube and HPC

$$\frac{\mathrm{d}m_{\mathrm{flv}}}{\mathrm{d}t}=\begin{cases}\dfrac{\varphi_{2\mathrm{v}}S_{\mathrm{v}}p_1}{\sqrt{f_1\tau_1}}K_0, & \text{if } \dfrac{p_1}{p_2}\ge k_{\mathrm{crit}}\\[2ex] \dfrac{\varphi_{2\mathrm{v}}S_{\mathrm{v}}p_1}{\sqrt{f_1\tau_1}}\sqrt{\dfrac{2k_0}{k_0-1}\left[\left(\dfrac{p_2}{p_1}\right)^{\frac{2}{k_0}}-\left(\dfrac{p_2}{p_1}\right)^{\frac{k_0+1}{k_0}}\right]}, & \text{if } 1<\dfrac{p_1}{p_2}<k_{\mathrm{crit}}\\[2ex] -\dfrac{\varphi_{2\mathrm{v}}S_{\mathrm{v}}p_2}{\sqrt{f_2\tau_2}}K_0, & if\ \dfrac{p_2}{p_1}\ge k_{\mathrm{crit}}\\[2ex] -\dfrac{\varphi_{2\mathrm{v}}S_{\mathrm{v}}p_2}{\sqrt{f_2\tau_2}}\sqrt{\dfrac{2k_0}{k_0-1}\left[\left(\dfrac{p_1}{p_2}\right)^{\frac{2}{k_0}}-\left(\dfrac{p_1}{p_2}\right)^{\frac{k_0+1}{k_0}}\right]}, & \text{if } 1<\dfrac{p_2}{p_1}<k_{\mathrm{crit}}\\[2ex] 0, & \text{if } p_1=p_2\end{cases} \tag{3}$$

- equation of mass

$$\frac{\mathrm{d}m_{g1}}{\mathrm{d}t}=\omega_1\frac{\mathrm{d}\psi_1}{\mathrm{d}t}-\frac{\mathrm{d}m_{\mathrm{flv}}}{\mathrm{d}t} \tag{4}$$

- equation of energy

$$\frac{\mathrm{d}\tau_1}{\mathrm{d}t}=\begin{cases}\dfrac{(1-\tau_1)f_1\omega_1\dfrac{\mathrm{d}\psi_1}{\mathrm{d}t}}{f_1m_{g1}}, & \text{if } p_1\ge p_2\\[3ex] \dfrac{(1-\tau_1)f_1\omega_1\dfrac{\mathrm{d}\psi_1}{\mathrm{d}t}-(f_2\tau_2-f_1\tau_1)\dfrac{\mathrm{d}m_{\mathrm{flv}}}{\mathrm{d}t}}{f_1m_{g1}}, & \text{if } p_1<p_2\end{cases} \tag{5}$$

- equation of state

$$p_1=\frac{f_1\tau_1m_{g1}}{W_{01}-\dfrac{\omega_1}{\delta_1}(1-\psi_1)-\alpha_1m_{g1}} \tag{6}$$

The following symbols are used in the preceding equation: χ_1, λ_1, μ_1 are the shape characteristics of powder grain; z_1 is the relative burnt thickness of grain; ψ_1 is the relative burnt igniter propellant mass; α_1, δ_1, ω_1 are the co-volume, density, and mas of igniter charge; I_{k1} is the total impulse of propellant gas; f_1 is the specific energy of igniter charge; T_{bd}, T_{tc1} are initial temperature and standard temperature of igniter charge; S_{v} is the total area of vents; p_1, p_2 are gas pressure in igniter tube and HPC; $\varphi_{2\mathrm{v}}$ is the correction factor; W_{01} is the initial volume of igniter tube; k_0 is the ratio of the specific heat.

The relative temperatures of the gas in the igniter tube and HPC are given by:

$$\tau_1=\frac{T_1}{T_{\mathrm{c}1}};\ \tau_2=\frac{T_2}{T_{\mathrm{c}2}}$$

where T_1, T_2 are the gas temperatures in the igniter tube and HPC; $T_{\mathrm{c}1}$, $T_{\mathrm{c}2}$ are the basic propellant combustion temperatures of igniter charge and propellant charge.

The equations in HPC:

$$\frac{\mathrm{d}z_2}{\mathrm{d}t} = \frac{\left[1 - k_{\mathrm{t}2}\left(T_{\mathrm{bd}} - T_{\mathrm{tc}2}\right)\right]^{-1}}{I_{\mathrm{k}2}} p_2 \tag{7}$$

$$\frac{\mathrm{d}\psi_2}{\mathrm{d}t} = \chi_2\left(1 + 2\lambda_2 z_2 + 3\mu_2 z_2^{\,2}\right)\frac{\mathrm{d}z_2}{\mathrm{d}t} \tag{8}$$

$$\frac{\mathrm{d}m_{fl1}}{\mathrm{d}t} = \begin{cases} \dfrac{\varphi_{21} S_1 p_2}{\sqrt{f_2 \tau_c}} K_0, & \text{if } \dfrac{p_2}{p_3} \geq k_{\mathrm{crit}} \\ \dfrac{\varphi_{21} S_1 p_2}{\sqrt{f_2 \tau_c}} \sqrt{\dfrac{2k_0}{k_0 - 1}\left[\left(\dfrac{p_3}{p_2}\right)^{\frac{2}{k_0}} - \left(\dfrac{p_3}{p_2}\right)^{\frac{k_0+1}{k_0}}\right]}, & \text{if } 1 < \dfrac{p_2}{p_3} < k_{\mathrm{crit}} \\ -\dfrac{\varphi_{21} S_1 p_3}{\sqrt{f_2 \tau_t}} K_0, & \text{if } \dfrac{p_3}{p_2} \geq k_{\mathrm{crit}} \\ -\dfrac{\varphi_{21} S_1 p_3}{\sqrt{f_2 \tau_t}} \sqrt{\dfrac{2k_0}{k_0 - 1}\left[\left(\dfrac{p_2}{p_3}\right)^{\frac{2}{k_0}} - \left(\dfrac{p_2}{p_3}\right)^{\frac{k_0+1}{k_0}}\right]}, & \text{if } 1 < \dfrac{p_3}{p_2} < k_{\mathrm{crit}} \\ 0, & \text{if } p_2 = p_3 \end{cases} \tag{9}$$

$$\frac{\mathrm{d}m_{fl2}}{\mathrm{d}t} = \begin{cases} \dfrac{\varphi_{22} S_2 p_2}{\sqrt{f_2 \tau_2}} K_0, & \text{if } \dfrac{p_2}{p_{kk}} \geq k_{\mathrm{crit}} \\ \dfrac{\varphi_{22} S_2 p_2}{\sqrt{f_2 \tau_2}} \sqrt{\dfrac{2k_0}{k_0 - 1}\left[\left(\dfrac{p_{\mathrm{a}}}{p_2}\right)^{\frac{2}{k_0}} - \left(\dfrac{p_{\mathrm{a}}}{p_2}\right)^{\frac{k_0+1}{k_0}}\right]}, & \text{if } 1 < \dfrac{p_2}{p_{kk}} < k_{\mathrm{crit}} \end{cases} \tag{10}$$

$$\frac{\mathrm{d}m_{fl3}}{\mathrm{d}t} = \begin{cases} \dfrac{\varphi_{23} S_3 p_2}{\sqrt{f_2 \tau_2}} K_0, & \text{if } \dfrac{p_2}{p_{\mathrm{a}}} \geq k_{\mathrm{crit}} \\ \dfrac{\varphi_{23} S_3 p_2}{\sqrt{f_2 \tau_2}} \sqrt{\dfrac{2k_0}{k_0 - 1}\left[\left(\dfrac{p_{\mathrm{a}}}{p_2}\right)^{\frac{2}{k_0}} - \left(\dfrac{p_{\mathrm{a}}}{p_2}\right)^{\frac{k_0+1}{k_0}}\right]}, & \text{if } 1 < \dfrac{p_2}{p_{\mathrm{a}}} < k_{\mathrm{crit}} \end{cases} \tag{11}$$

$$\frac{\mathrm{d}m_{g2}}{\mathrm{d}t} = \omega_2 \frac{\mathrm{d}\psi_2}{\mathrm{d}t} - \frac{\mathrm{d}m_{fl1}}{\mathrm{d}t} - \frac{\mathrm{d}m_{fl2}}{\mathrm{d}t} - \frac{\mathrm{d}m_{fl3}}{\mathrm{d}t} \tag{12}$$

$$\frac{\mathrm{d}\tau_2}{\mathrm{d}t} = \begin{cases} \dfrac{\left(1 - \tau_2\right)\omega_2 \dfrac{\mathrm{d}\psi_2}{\mathrm{d}t}}{m_{g2}}, & \text{if } p_2 \geq p_3 \\ \dfrac{\left(1 - \tau_2\right)\omega_2 \dfrac{\mathrm{d}\psi_2}{\mathrm{d}t} - \left(\tau_3 - \tau_2\right)\dfrac{\mathrm{d}m_{fl1}}{\mathrm{d}t}}{m_{g2}}, & \text{if } p_2 < p_3 \end{cases} \tag{13}$$

$$p_2 = \frac{f_2 \tau_2 m_{g2}}{W_{02} - \frac{\omega_2}{\delta_2}(1-\psi_2) - \alpha_2 m_{g2}} \tag{14}$$

where χ_2, λ_2, μ_2 are the shape characteristic parameters of the powder grain; z_2 is the relative burnt thickness of grain; ψ_2 is the relative burnt propellant mass; α_2, δ_2, ω_2 are the co-volume, density, and mas of propellant charge; I_{k2} is the total impulse of propellant gas; f_2 is the specific energy of propellant charge; $T_{bd,}$ T_{tc2} are initial temperature and standard temperature of propellant charge; $p_{3,}$ p_a are gas pressure in LPC and atmospheric pressure; φ_{21}, φ_{22}, φ_{23} is the correction factor; W_{02} is the initial volume of HPC. S_1, S_2, and S_3 are the total critical areas of nozzles 1, 2, and 3, respectively.

The relative gas temperature in the LPC is given by:

$$\tau_3 = \frac{T_3}{T_{c2}}$$

where T_3 is the gas temperature in the LPC.

The equations in LPC:

$$\frac{\mathrm{d}m_{flg}}{\mathrm{d}t} = \begin{cases} \frac{\varphi_{2g} S_g p_3}{\sqrt{f_2 \tau_3}} K_0, & \text{if } \frac{p_3}{p_a} \geq k_{crit} \\ \frac{\varphi_{2g} S_g p_3}{\sqrt{f_2 \tau_3}} \sqrt{\frac{2k_0}{k_0 - 1}\left[\left(\frac{p_a}{p_3}\right)^{\frac{2}{k_0}} - \left(\frac{p_a}{p_3}\right)^{\frac{k_0+1}{k_0}}\right]}, & \text{if } 1 < \frac{p_3}{p_a} < k_{crit} \end{cases} \tag{15}$$

$$\frac{\mathrm{d}m_{g3}}{\mathrm{d}t} = \frac{\mathrm{d}m_{fl1}}{\mathrm{d}t} - \frac{\mathrm{d}m_{flg}}{\mathrm{d}t} \tag{16}$$

$$\frac{\mathrm{d}\tau_3}{\mathrm{d}t} = \begin{cases} \frac{(\tau_2 - \tau_3)\mathrm{d}m_{fl1} - \frac{k_0 - 1}{k_0 f_2}\varphi m v \mathrm{d}v}{m_{g3}}, & \text{if } p_2 \geq p_3 \\ \frac{-\frac{k_0 - 1}{k_0 f_2}\varphi m v \mathrm{d}v}{m_{g3}}, & \text{if } p_2 < p_3 \end{cases} \tag{17}$$

$$p_3 = \frac{f_2 \tau_3 m_{g3}}{W_{03} - \alpha_2 m_{g3} + S_n L} \tag{18}$$

$$\frac{\mathrm{d}v}{\mathrm{d}t} = \frac{S_n (p_3 - p_4)}{\varphi m} \tag{19}$$

$$\frac{\mathrm{d}L}{\mathrm{d}t} = v \tag{20}$$

Equation of state in chamber Nr. 4:

$$p_4 = \begin{cases} \dfrac{p_a W_{04}}{W_{04} - S_n L}, & \text{if } p_4 \le p_{br} \\ p_a, & \text{if } p_4 > p_{br} \end{cases} \tag{21}$$

where S_g denotes the leakage area between the grenade and launcher tube; φ_{2g} is the correction factor; W_{03}, W_{04} are the initial volumes of LPC and m is the grenade mass; φ is the coefficient of fictitious grenade mass; v is the grenade velocity; S_n is the cross-sectional area of barrel; L is the grenade path in barrel; p_{br} is the value of the pressure that will cause bursting of the cap.

3 Calculation Results

The system of equations consists of first-order ordinary differential equations and algebraic equations, from Eqs (1) to (21). Using the fourth-order Runge-Kutta method, numerical integration software has been developed to determine the gas pressure changes in the igniter tube, HPC, LPC, and the grenade velocity over time. The calculations were performed for a 93 mm recoilless gun, the design parameters of which are given in Tab. 1.

Tab. 1 Design parameter of recoilless weapon 93 mm

Parameters	**Signification**	**Value**	**Parameters**	**Signification**	**Value**
Caliber [m]	D	0.093	Propellant mass [kg]	ω_1	0.0145
The maximum distance travel of grenade within the barrel [m]	L_n	0.636		ω_2	0.34
Cross-sectional area of barrel bore [m^2]	S_n	0.0068	Specific energy of propellant charge [J/kg]	f_1	265 035
Cross-sectional area critical of nozzle [m^2]	S_1	1.43×10^{-4}		f_1	857 982
	S_2	9.81×10^{-4}	Total pressure impulse of propellant gases [Pa·s]	I_{k1}	180×10^3
	S_3	4.73×10^{-4}		I_{k2}	350×10^3
Total area of vents [m^2]	S_v	8.03×10^{-5}	Covolume of propellant gas [m^3/kg]	$\alpha_1 = \alpha_2$	1.24×10^{-3}
Cross-sectional area gap [m^2]	S_g	3.36×10^{-5}	Density of propellant charge [kg/m^3]	$\delta_1 = \delta_2$	1 540
Grenade mass [kg]	M	3.94	Geometric characteristics of powder grain	$\chi_1; \lambda_1; \mu_1$	3; −1; 1/3
Chamber initial volume [m^3]	W_{01}	1.47×10^{-5}		$\chi_2; \lambda_2; \mu_2$	1.036; 0.0036; 0
	W_{02}	6.04×10^{-4}	Specific heat ratio	k_0	122
	W_{03}	4.47×10^{-4}	Atmosphere pressure [Pa]	p_a	1×10^5
	W_{04}	1.40×10^{-3}	Initial temperature [°C]	T_{bd}	5 and 50

The results of the solution for the two cases where the initial temperature of the propellant charge is 5 °C and 50 °C are shown in Tab. 2 and Figs 3 and 4.

Tab. 2 Results of solution

No.	Initial temperature of propellant	p_{1max} [MPa]	p_{2max} [MPa]	p_{3max} [MPa]	V_0 [m/s]	$\frac{p_{1max}}{p_{3max}}$	$\frac{p_{2max}}{p_{3max}}$
1	5 °C	170.68	53.95	13.06	124.6	13.07	4.13
2	50 °C	207.54	59.00	14.66	129.9	14.16	4.02

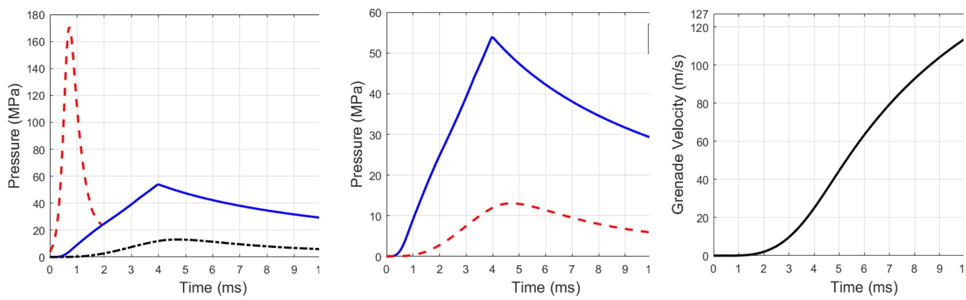

a) *b)* *c)*

Fig. 3 Pressure in igniter tube, HPC and LPC vs time (a), (b) and velocity of grenade plot vs time (c) when temperature of the propellant is 5 °C

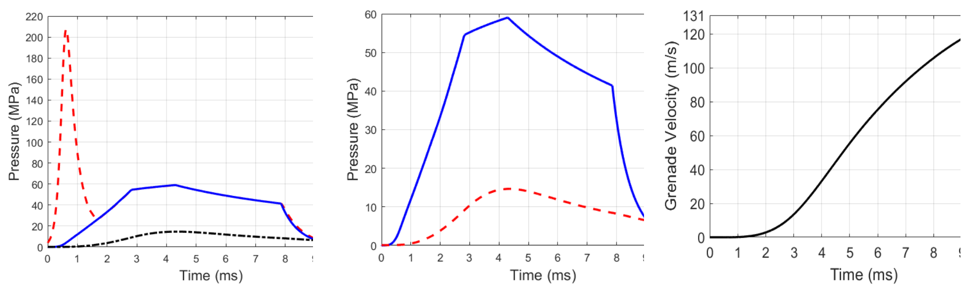

a) *b)* *c)*

Fig. 4 Pressure in igniter tube, HPC and LPC plots vs time (a), (b) and velocity of grenade plot vs time (c) when temperature of the propellant is 50 °C

4 Experimental Verification

To verify the mathematical model, an experiment was conducted (Fig. 5). The test apparatus includes a firing tube (2), a cartridge with a HPC (5), a simulated grenade (3) and a joint (4). The temperature of the propellant charge before firing was 5 °C and 50 °C.

The grenade velocity was measured using a DRS-1 Doppler radar system with a flame detector used as a trigger to start the measurement. Kistler 6215 piezoelectric pressure transducers were used to simultaneously record the pressure inside both HPC and LPC.

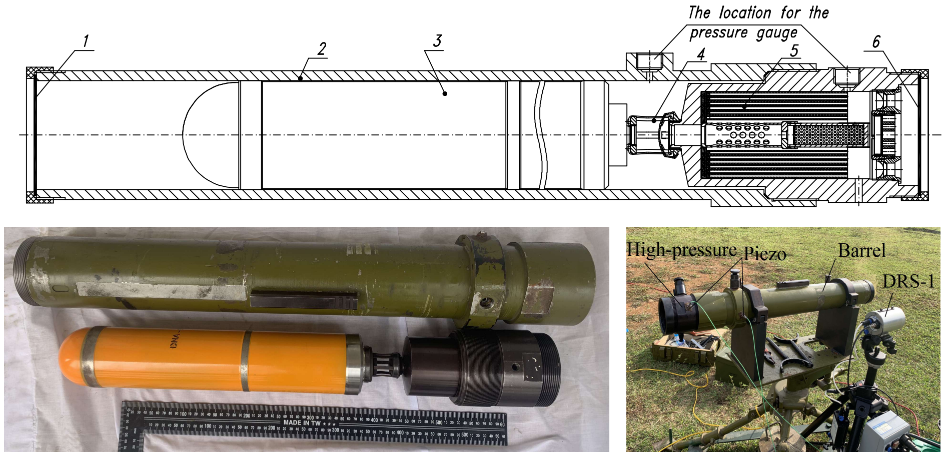

Fig. 5 The experimental setup

The experiment results are presented in Tabs 3 and 4 and Fig. 6.

Tab. 3 Experiment data when temperature of the propellant charge was 5 °C

No.	p_{2max} [MPa]	p_{3max} [MPa]	V_0 [m/s]
1	57.59	13.31	125.2
2	56.60	13.60	126.3
3	52.40	14.20	125.6
4	52.70	14.10	124.8
5	42.90	14.64	123.9
6	39.17	12.88	119.7
7	48.57	14.37	122.0
Average	**49.99**	**13.87**	**123.9**

Tab. 4 Experiment data when temperature of the propellant charge was 50 °C

No.	p_{2max} [MPa]	p_{3max} [MPa]	V_0 [m/s]
1	56.54	14.11	129.0
2	63.88	15.67	129.7
3	64.29	15.57	125.7
4	50.39	14.19	128.2
5	57.87	13.31	126.5
6	59.01	14.69	129.9
Average	**58.66**	**14.59**	**128.2**

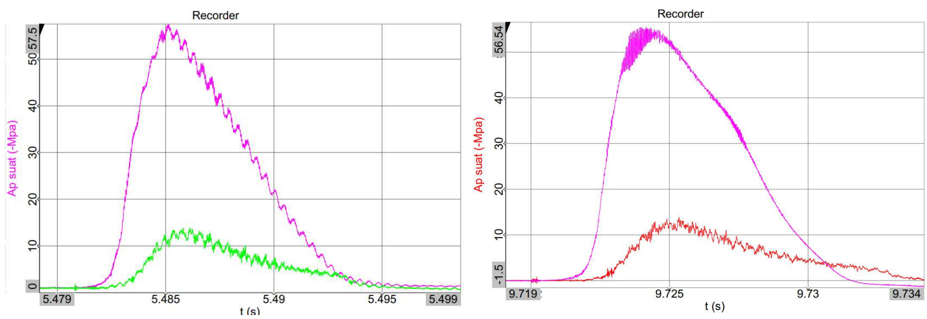

a) *b)*

Fig. 6 Experiment result of pressure in HPC and LPC plots vs time when temperature of the propellant charge was 5 °C *(a) and* 50 °C *(b)*

Tab. 5 provides a quantitative comparison of the maximum pressure and velocity values obtained through numerical simulation and experimental testing. The high degree of agreement between the two sets of data substantiates the accuracy of the mathematical model.

Tab. 5 Computational-experimental comparison

Parameters	Calculation	Experiment	Difference	Note
p_{2max}. [MPa]	53.95	49.99	7.92 %	5 °C
p_{3max}. [MPa]	13.06	13.87	5.84 %	
V_0. [m/s]	124.6	123.9	0.56 %	
p_{2max}. [MPa]	59.00	58.66	0.58 %	50 °C
p_{3max}. [MPa]	14.66	14.59	0.48 %	
V_0. [m/s]	129.9	128.2	1.33 %	

5 Conclusion

An internal ballistic mathematical model was developed for recoilless weapons in which the propellant gas flows out from HPC. The problem I has been solved using the numerical integration method in MATLAB software. The calculation results can determine the pressure variation inside the igniter tube over time, which is significant for igniter charge design. The results show that the maximum pressure values in the igniter tube and HPC are approximately 14 and 4 times higher than that in LPC, respectively. The mathematical model and experiment were used to determine the gas pressure in HPC, LPC, time and velocity of the grenade at the muzzle. By comparison, the difference between the result of the mathematical model and the value obtained by the experiment was found to be a maximum of 7.92 % (for p_{2max} value) for propellant charge temperature 5 °C and a maximum of 1.33 % (for v_0 value) for propellant charge temperature 50 °C.

Acknowledgement

The work presented in this paper has been supported by the Ministry of Defence of the Czech Republic (research project VAROPS, DZRO-FVT22-VAROPS).

References

[1] CARLUCCI, D.E. and S.S. JACOBSON. *Theory and Design of Guns and Ammunition*. 3rd ed. Boca Raton: CRC Press, 2018. ISBN 978-1-138-05531-5.

[2] PLIHAL, B., S. BEER, J. KOMENDA, L. JEDLICKA and B. KUDA. *Ballistics* (in Czech). Brno: University of Defence, 2011. ISBN 978-80-7231-785-7.

[3] PLIHAL, B., S. BEER and L. JEDLICKA. *Interior Ballistics of Gun Barrel: Collection of Examples and Exercises* (in Czech). Brno: University of Defence, 2005.

[4] BIEN, V.V., S. BEER, T.S. NGO and D.P. NGUYEN. The Effect of the Nozzle Ultimate Section Diameter on Interior Ballistics of HV-76 Trial Gun. In: *2019 International Conference on Military Technologies (ICMT)*. Brno: IEEE, 2019. DOI 10.1109/MILTECHS.2019.8870040.

[5] DOANH. V.T. Equation of Energy of the Internal Ballistic Model in the Jet Dynamic System. *Journal of Science and Technology*, 2012. ISSN 1859-1043.

[6] JARAMAZ, S., D. MICKOVIC, Z. ZIVKOVIC and R. CURCIC. Internal Ballistic Principle of High/Low Pressure Chambers in Automatic Grenade Launchers. In: *19th International Symposium of Ballistics*. Interlaken: International Ballistics Society, 2001. ISBN 978-3-9522178-4-9.

[7] VASILE, T., D. SAFTA and C. BARBU. Studies and Researchers Concerning Grenade Launcher with High-Low Pressure Chambers. *Problemy Techniki Uzbrojenia*, 2006, **35**, pp. 15-23. ISSN 1230-3801.

[8] DUNG., T.N. and D.D. LINH. Internal Ballistics of High-Low Pressure Decoy Launcher with a Secondary Propellant Charge. In: *International Conference on Military Technologies (ICMT) 2019*. Brno: IEEE, 2019. DOI 10.1109/MILTECHS. 2019.8870020.

[9] VI., D.Q., N.T. MINH, D.V. MINH and P.V. CUONG. Building a Model for the Internal Ballistic Problem of Recoilless Weapons with High-Pressure Combustion Chamber. *Journal of Military Science and Technology*, 2023, **92**(92), pp. 151-159. DOI 10.54939/1859-1043.j.mst.92.2023.151-159.